J Mater Sci (2007) 42:156–165
DOI 10.1007/s10853-006-1035-2

Nanotailoring photocrosslinkable epoxy resins with multi-walled carbon nanotubes for stereolithography layered manufacturing

J. H. Sandoval · K. F. Soto · L. E. Murr · R. B. Wicker

Received: 2 September 2005 / Accepted: 4 January 2006 / Published online: 9 December 2006

Abstract Exploiting nanostructured materials' characteristics and properties in stereolithography (SL) may open new markets for unique rapidly manufactured functional devices. Controlled amounts of multi-walled carbon nanotubes (MWCNTs) were successfully dispersed in SL epoxy-based resins and complex three-dimensional (3D) parts were successfully fabricated by means of a modified SL setup. The effect of the nanosized filler was evaluated by means of mechanical testing. Small concentrations of MWCNTs resulted in significant effects on the physical properties of the polymerized resin. A MWCNT concentration of 0.05% (w/v) increased the ultimate tensile stress and fracture stress an average of 17% and 37%, respectively. Increasing the MWCNT concentration to 0.5% (w/v) enhanced the integrity of the nanocomposite samples over much wider operating temperatures. Sample parts were characterized by scanning and transmission electron microscopy to measure the impact of this particular nanomaterial on the morphology of the nanocomposite samples and results showed affinity between the constituents and identified buckled nanotubes that illustrated strong interfacial bonding. These improved physical properties may provide opportunities for using nanocomposite SL resins in end-use applications. Varying types and concentrations of nanomaterials can be used to tailor existing SL resins for particular applications.

J. H. Sandoval (✉) · R. B. Wicker
W.M. Keck Border Biomedical Manufacturing and Engineering Laboratory, Department of Mechanical and Industrial Engineering, The University of Texas at El Paso, 500 W. University Ave. M&I Engineering E-108, El Paso, TX 79968, USA
e-mail: jhsandoval@utep.edu

K. F. Soto · L. E. Murr
Department of Metallurgical and Materials Engineering, The University of Texas at El Paso, El Paso, TX 79968, USA

Introduction

Recent advancements in the synthesis, processing and understanding of nanostructured materials have generated considerable interest in the materials research community. Since the discovery of carbon nanotubes (CNTs) in the early 90s, the scientific community has been investigating methods to fully exploit their properties. CNTs and more specifically single-walled CNTs are characterized by an exceptionally high aspect ratio (~1000:1), very low density, a high strength (tensile strength ~ 100 GPa), high stiffness (above 1,000 GPa) and the capability to conduct electricity (resistivity ~0.5 $\mu\Omega$m or less depending on tube diameter) [1]. These characteristics make CNTs ideal candidates for polymer-composite reinforcement. Dispersing CNTs in a polymer matrix could potentially increase the mechanical strength of the polymer, introduce electrical conductivity [2, 3] or simply improve the polymer's mechanical behavior and integrity at temperatures beyond its glass transition temperature (T_g).

The objective of this research was to investigate tailoring the mechanical and thermal properties of existing epoxy-based resins by dispersing controlled amounts of multi-walled carbon nanotubes (MWCNTs) in their polymeric matrix. These epoxy-based resins are used as build materials in one of the most popular and

accurate rapid prototyping (RP) systems: the stereolithography (SL) layered manufacturing process. The main motivation for this research was the development of a new class of high performance material for specific SL applications. This MWCNT-reinforced-polymer for SL holds considerable promise since adding this particular nanostructured material could potentially improve the properties of SL resins as well as expose this RP technology to a new variety of applications.

Background

Epoxy resins such as two-part epoxy adhesives are widely used in consumer products for the automotive, aerospace, and other industries. These well-known epoxy systems are normally thermally cured in the presence of amines, acid anhydrides and other types of catalysts. The possible enhancement of the physical and mechanical properties of two-part epoxy systems by CNT dispersions (concentrations above 1% (w/v)) is certainly not new and has been studied by other researchers [4–7]. Among the reported improvements are: the increase in tensile strength, increase in electrical conductivity, and an increase in the thermal conductivity of the epoxies. The test specimens used in these previous studies were either cast or went through injection molding to achieve their final shape. Furthermore, once the specimens were fabricated, they were post-processed to completely cure the epoxy-based nanocomposite (which often took up to 24 h). In the present research, UV photocurable SL resins (formulated from photoinitiators and reactive liquid monomers) are used as the nanocomposite matrix with MWCNTs as the reinforcing agents. Thus, this technique takes advantage of the accuracy and build speed that characterize SL and requires minimal post-processing. Furthermore, this technique allows the user to build complex 3D nanocomposite geometries, which cannot be fabricated by other means.

Experimental setup and procedures

Materials and equipment

Commercially available epoxy-based SL resins, DSM Somos® WaterClear™ and WaterShed™ were used as the nanocomposite's matrix materials. These resins undergo a cationically activated polymerization process, which is initiated by rastering a UV laser over the surface of the resin. The interested reader may gain further understanding of these systems elsewhere [8, 9].

The MWCNTs used in this research (nanocomposite's filler) were produced by a chemical vapor deposition (CVD) process using a ceramic oxide support. The MWCNTs were then purified by means of acid etching to 95% (by mass). According to the manufacturer (NanoLab, Inc. Newton, MA), the MWCNTs were characterized by a mean outer diameter of 30 ± 15 nm and a length of 5–20 microns, which represents an actual surface area of ~220 m^2 per gram of nanotubes. A sample of MWCNTs was prepared on silicon monoxide/formvar-coated Cu mesh grids and examined under transmission electron microscopy (TEM): a Hitachi H-8000 analytical TEM fitted with a Noran energy-dispersive (X-ray) spectrometer (EDS) system with a goniometer-tilt stage, operated at 200 kV accelerating potential. A TEM micrograph of the purchased raw material and its diffraction pattern were obtained to verify that the materials used in this project were indeed MWCNTs as specified above (Fig. 1) [10].

A modified 3D Systems SL machine (Model 250/50) equipped with a DPSS laser upgrade (wavelength 355 nm) was used in this study. The modifications consisted of removing the sweeping mechanism and the original ~46 L vat of material and retrofitting a rotating multi-vat carousel system. The rotating vat carousel is composed of three vats (each ~750 mL) distributed circumferentially and attached to a manual rotary stage via a shaft. The original 25.4 cm by 25.4 cm platform was replaced with a smaller 11.4 cm by 11.4 cm platform, which was attached to the z-stage via an extended assembly. The center of the smaller platform remained in the center of the build envelope so that the laser's starting location remained unchanged. The vats contained a partition that served to

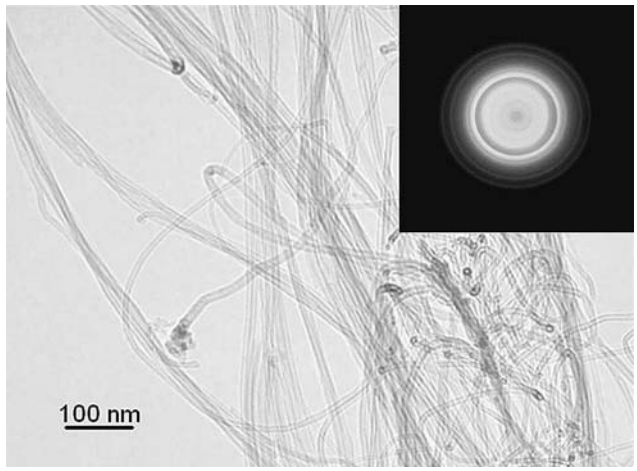

Fig. 1 TEM micrograph and diffraction pattern of MWCNTs

separate the main vat chamber from a second overfill vat chamber. This partition also served to maintain a constant resin liquid level by continuously pumping the liquid nanocomposite into the main vat chamber using a peristaltic pump (Masterflex L/S, Model 7550-30). This recirculation system was crucial for a successful part build since this modified system was not equipped with a recoating or sweeping mechanism (more complete details of this system can be found in [11, 12]).

Procedure

The MWCNTs were used as supplied and directly seeded in the SL resins to the desired concentrations by means of shear and ultrasonic dispersion. The mixture was first stirred mechanically via a paddle until visual uniformity was achieved. Then, the mixture was ultrasonicated for ~1 h to diminish the formation of MWCNTs agglomerates. Although several researchers have reported negative effects of ultrasonic dispersion on CNTs, most of the reported work [2, 3, 13] has been performed by means of an ultrasonic gun. Once the gun is inserted in the low viscosity CNT solution (liquid dispersing agent solution with ~1.2 cPs at 20 °C), it breaks the bundled structures through its localized ultrasonic effect. However, this dispersion technique is only temporary and the agglomerates form again, since the CNTs' attractive forces become active shortly after the gun is removed. Moreover, there have been reports that localized ultrasonic dispersion physically damages the CNTs structure (i.e., reduces their effective length) [13]. The ultrasonic dispersion technique used in this research was non-localized, and the viscosity of the resins utilized were ~130 for WaterClear™ and ~260 cPs at 30 °C for WaterShed™. Thus, any negative ultrasonic effects were diminished. In other words, the solutions held a colloidal state for a prolonged period (at least one week) as no precipitation was observed in the solution. This is mainly attributed to the high viscosity of the SL epoxy resins, which overcomes the attractive forces between CNTs and delays the formation of CNT agglomerates, and thus, their precipitation. Moreover, since the ultrasonic dispersion was non-localized, the CNTs' effective length was not directly affected. Once the nanocomposite was ultrasonicated for ~1 h, the nanocomposite was poured into a vat to manufacture sample parts by selectively curing it to a prescribed geometry using standard SL manufacturing in the multi-material SL machine. The peristaltic pump was set to run at 10 mL/min to maintain a constant resin level and to provide means for a mechanical, constant mixing and steady recirculation of the nanocomposite. This was one of the main advantages of this modified system as it helped ensure a well-mixed nanocomposite and that no large MWCNT agglomerates were formed. Figure 2 depicts a comparison of pure (semi-transparent) SL resin and the same resin containing 0.05% (w/v) of MWCNTs (opaque) [10].

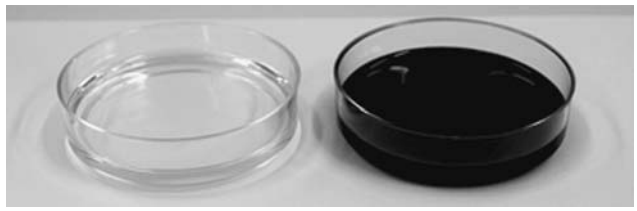

Fig. 2 Petri dishes containing pure WaterShed™ (left) and WaterShed™ with 0.05wt% (w/v) of MWCNTs

Results and discussion

A sample of the SL nanocomposite (~150 mL) was prepared as described previously by mixing the epoxy resin and MWCNTs at a concentration of 0.5% (w/v). Once rectangular specimens were manufactured and cleaned with isopropyl alcohol, it was observed that uneven photopolymerization occurred. In other words, the upfacing surface of the rectangular specimen exhibited a glossy finish (Fig. 3b), whereas the downface exhibited a dull and rough finish. Furthermore, the specimens also experienced part curling. Part curling can be attributed to two factors. First, it is well known that, if the laser's cure depth is too great, internal stresses can build up until they reach a critical level that may cause layer curling.

This phenomenon is further enhanced by the poor mechanical strength that characterizes SL parts in a green state (partially polymerized) [8, 9]. Without sufficient green strength, the viscous forces generated during the part-building stage of the process, along with factors such as gravity and more specifically the change in density of the material upon polymerization (downward force) may result in part delamination and other distortions. Secondly, as a result of seeding the MWCNTs in the SL epoxy resin, there was a significant increase in surface tension of the resin due to the large surface area (~220 m^2 per gram of MWCNTs) of the CNTs, which is one of the most fascinating aspects of nanomaterials.

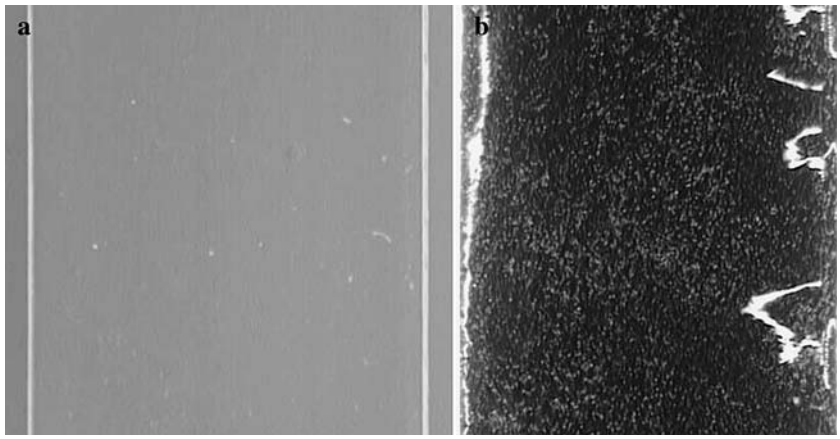

Fig. 3 Pure SL epoxy resin specimen (**a**) the sample is characterized for being clear and it does not experience part curling. (**b**) MWCNTs/SL resin nanocomposite sample (notice the change in color due to the presence of MWCNTs)

SEM characterization

Surface finish differences between the up-face (glossy or mirror finish Fig. 4a), down-face (dull and rough finish, Fig. 4b) and side faces (layered finish Fig. 4c) of 3D SL parts are a common occurrence and can be appreciated in the environmental scanning electron microscope (ESEM) scans of Fig. 4 taken from a sample of WaterClear^{TM} resin without MWCNTs [14]. As mentioned before, SL is a layer based technology and thus, differences in the finish are mainly produced by constraints upon polymerization. When a part is first ''attached'' to the SL machine's platform, the first layer of liquid resin is cured, polymerized, or solidified and the polymer's movement is restricted by the presence of the metallic platform or other types of support structures. Thereafter, when subsequent layers are solidified, their movement is only restricted by previous layers, which are in a green or more flexible state (i.e., not fully polymerized).

As mentioned before, gravity effects also impact the surface quality of solidified layers since the density of

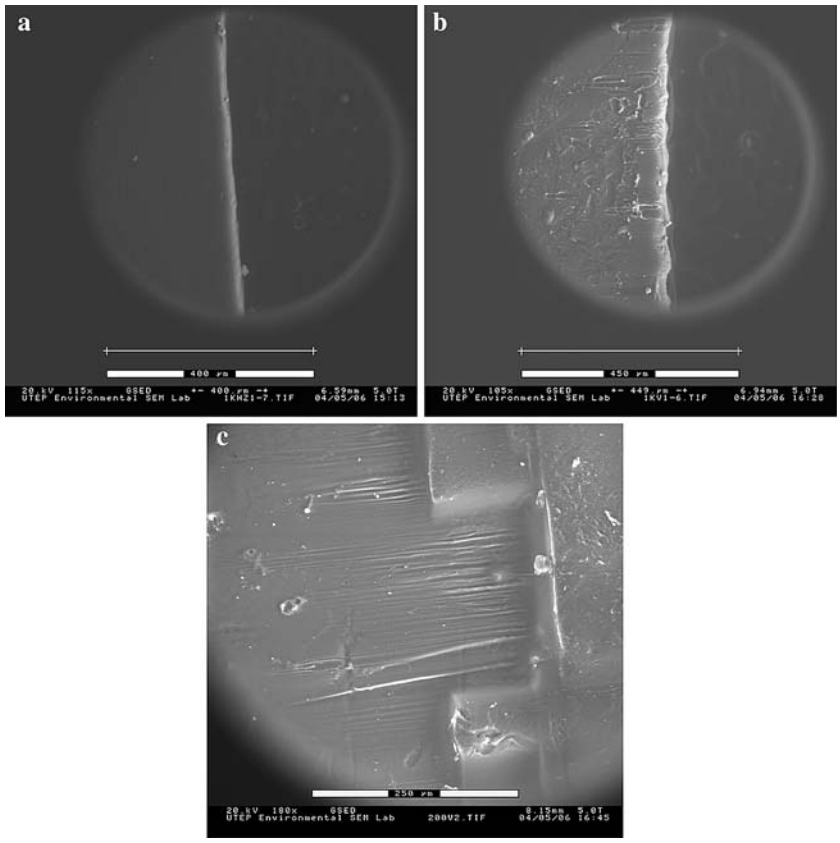

Fig. 4 ESEM micrographs taken from the up-face (**a**), down-face (**b**) and lateral face (**c**) of a specimen manufactured with pure SL epoxy resin. The surface finish differences can be appreciated from these scans

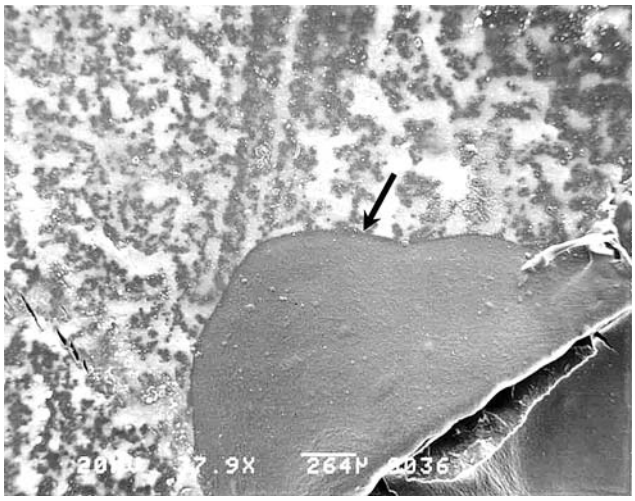

Fig. 5 SEM micrograph showing the up-face surface of the sample (the arrow denotes the graphite paint used to ground the sample)

the build material increases with the degree of polymerization. The last (topmost or up-face) layer is the one in direct contact with the free surface (unconstrained) and thus is the one that exhibits the smoothest and glossiest finish. It is believed that all these constraints contribute to the buildup of internal stresses (within layers), which can affect not only the surface finish but the amount of detail that can be achieved on SL parts. Nonetheless, the differences in surface finish (up and down faces) and the part curling of the nanocomposite samples were very intriguing. Samples were gold-coated, glued and grounded to an aluminum sample holder with graphite paint and then observed in a scanning electron microscope (SEM), an ISI DS130 at 20 kV. It was observed that the sample's up-face surface was smooth and cured uniformly as seen in Fig. 5.

However, when the down-face of the samples was analyzed, a totally unexpected morphology was observed. As a result of the presence of MWCNTs in the SL resin, the sample's surface was greatly impacted by a ''wrinkling effect'' which is shown in Fig. 6a, b, c and d. Furthermore, as seen in the previously described ESEM scans (Fig. 4), this morphology does not exist in unreinforced or pure SL resins.

As mentioned before, there was an increase in the surface tension effects due to the large surface area of the nanotubes, which explains the significant impact of reinforcing SL resins with small amounts of MWCNTs (0.5% (w/v)) on the surface morphology. Although the viscosity of the resin is somewhat high (~130 cPs at 30 °C), the attractive forces between graphitic structures of the nanotubes were still active; thus, the nanotubes grouped into long fiber-like structures. Subsequently, the liquid polymer was absorbed by these structures and once the photopolymerization process started, the resin solidified by wrapping around these groups and resulted in the wrinkling of the sample's surface. The CNTs attractive forces are mainly produced by extended π electron systems; these systems are highly polarizable and thus, are subject to van der Waals force interactions [1]. These interactions

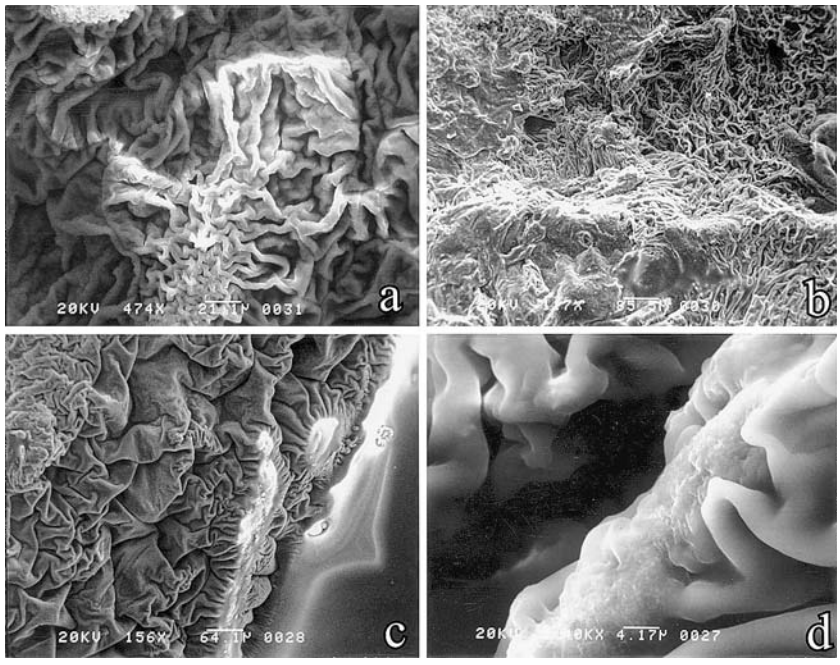

Fig. 6 SEM micrographs taken from the down-face of the sample. These micrographs show the significant effect of the MWCNTs on the morphology of SL parts (**a** & **b**). SEM micrographs taken at the edge of the MWCNTs/SL resin nanocomposite sample (**c** & **d**)

induce the formation of nanotubes agglomerates or, in this case, the fiber-like groups while the nanotubes were suspended in the liquid resin. To further investigate the effect of even smaller concentrations of MWCNTs, a second sample of the nanocomposite was prepared at a concentration of 0.05% (w/v). The manufactured specimens were characterized as described before but no significant deformations were observed on the morphology of the surface of the specimens, since it resembled the surface finish of unreinforced SL resin parts (Fig. 4).

Dynamic mechanical analysis testing

The dynamic mechanical analysis (DMA) technique was used to characterize the nanocomposite's dynamic mechanical properties and response over a wide temperature range [15]. The nanocomposite samples were manufactured as described before (at a concentration of 0.5% (w/v)) and subjected to a controlled temperature program and oscillatory loads as per ASTM E1640-99 using a DMA Q800, from TA Instruments. This method was used to approximate the glass transition temperature of the nanocomposite by measuring the change in modulus observed in going from the hard, brittle region to the soft, rubbery region while ramping the temperature in a controlled environment [15–17, 21]. This test consisted of placing the nanocomposite rectangular specimens (60 mm × 12 mm × 0.5 mm) in a dual cantilever beam sample holder, applying a constant strain, and ramping the temperature from room temperature to ~300 °C at a rate of 1 °C per minute.

Although no changes in the glass transition temperature between the pure resin sample and the nanocomposite at a MWCNT concentration of 0.5% (w/v) were observed. The nanocomposite samples exhibited an impact in the storage modulus (E') by first decreasing from ~24,000 MPa (for unreinforced WaterClear™) to ~8,000 MPa (for the nanocomposite) (Fig. 7). While the storage modulus of the pure SL resin has been reduced, the nanocomposite (at a MWCNT concentration of 0.5% (w/v)) sample exhibits an increase in elasticity starting at ~75 °C and up to a maximum of ~11,000 MPa at ~220 °C. This second phase is attributed to the reinforcing action of the nanotubes in the molecular structure of the crosslinked chains. The nanocomposite samples showed a considerable improvement of their integral mechanical properties at high temperatures. The mechanisms for this behavior are currently being explored. Other studies [1, 2] have shown the benefits of dispersing nanotubes in similar epoxy

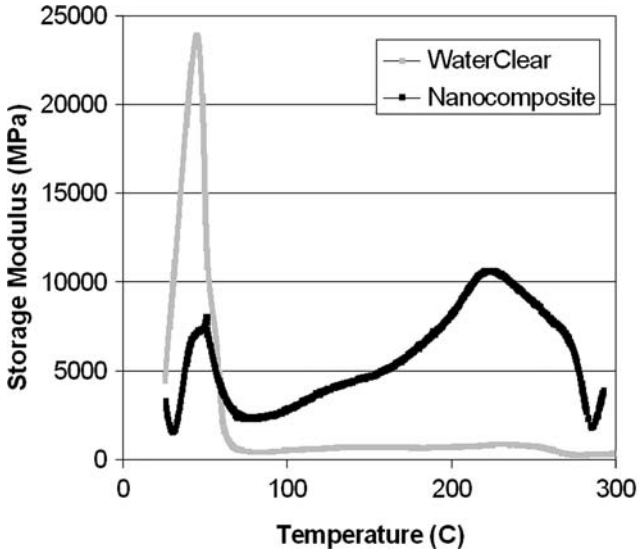

Fig. 7 Storage modulus plot obtained during the glass transition temperature test of the MWCNTs/SL resin nanocomposite test specimen

systems at temperatures above the glass transition temperature of the material. It is believed that the MWCNTs served as means to dissipate heat evenly throughout the sample (acting as nano-scaled heat sinks) and allowed the SL nanocomposite sample's structure to accommodate accordingly to the demanding changes occurring during the dynamic test. MWCNT dispersion-strengthened composites could open new SL markets for high temperature testing applications and other end-use applications.

Mechanical testing

To measure the effect of dispersing MWCNTs on the mechanical properties of the SL resin, nanocomposite tensile test specimens and control samples (pure SL resin) were manufactured as per ASTM D-638 [18] (type V specimen) in the multi-material setup described previously (see Fig. 8). The nanocomposite specimens were mechanically tested for ultimate tensile stress, fracture stress (or breaking strength), and fracture strain (or elongation at break) and hardness. The tensile specimens were cleaned with isopropyl alcohol and post-cured in a UV oven for ~1 h (~30 min each side). To further investigate the effect of this particular nanostructure material on the resin, microhardness measurements were taken from the samples prior to mechanical testing.

Tensile testing was performed with an INSTRON 5500 machine and the cross-head speed during testing

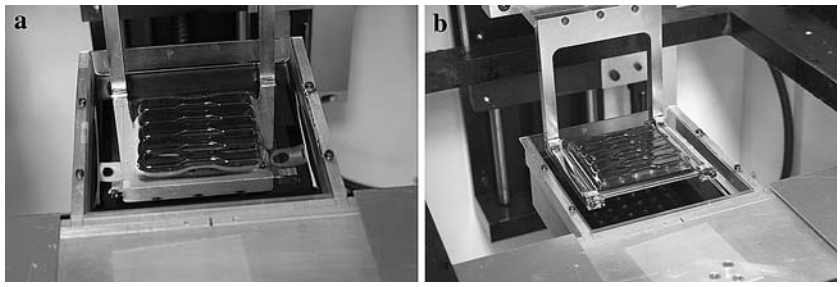

Fig. 8 Building of tensile test samples: (**a**) WaterShed™, and (**b**) WaterShed™ with 0.05% (w/v) MWCNTs

was set at 10 mm/min [10]. Table 1 shows a summary of the test results for pure SL resin and the nanocomposite containing 0.05% (w/v) of MWCNTs.

The micro-hardness testing showed an increase from 13 to 16 VHN in the hardness number (Vickers scale) of the nanocomposite when compared to pure SL resin. Concurring with the hardness increase, an average increase of ~17% on the ultimate tensile stress and an increase of ~37% on the fracture or breaking stress was observed in the tested specimens. The stress–strain curves reflect a repeatable behavior. Figure 9 portrays an increase in the mechanical strength of the nanocomposite when compared to the control samples. The strengthening mechanisms are attributed to an assisted adhesion between layers due to the random orientation and distribution of the nanotubes (embedded within the polymer chains) and a reduction in the mobility of the chains upon deformation. These improvements also suggest an effective load transfer via shearing mechanisms and strong interface bonding between the highly crosslinked matrix to the randomly distributed filler which delays fracture mechanisms. The increase in hardness with the addition of MWCNTs might be explained on the basis of the high stiffness of the nanotubes (typically above 1,000 GPa [1]), which reinforces not only the specimen's structure but its surface.

However, the nanocomposite specimens experienced a fracture strain decrease of ~30%. As depicted in Fig. 9a, there has been a drastic reduction in the plastic region shown in the nanocomposite's stress versus strain curves. This reduction resulted in a brittle type fracture mode for the nanocomposite specimens. The brittle fracture mode is a result of the constraints imposed by the nanotubes in the polymer chain movement upon deformation. This is further supported by the ductile fracture mode observed in the control samples, where signs of macroscopic plastic deformation were observed on the tested specimens.

Table 1 Mechanical testing results

Material	Ultimate tensile stress (MPa)	Standard deviation (MPa)	Fracture stress (MPa)	Standard deviation (MPa)	Fracture strain (mm/mm)
WaterShed 11120	42	1	29	1	0.14
WaterShed 11120/ MWCNTs (0.05wt%)	51	>1	46	4	0.10

TEM characterization

To investigate the interface between the MWCNTs and the SL resins in this novel nanocomposite, samples from the fracture surface of the tensile test specimens were characterized under TEM. The nanocomposite samples (both concentrations) were

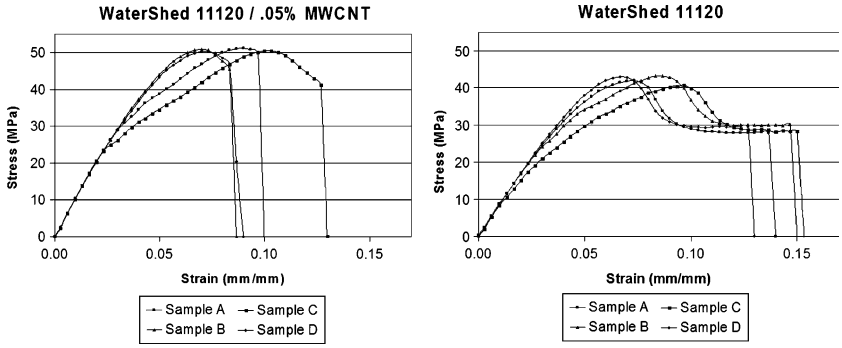

Fig. 9 Stress versus strain results: WaterShed™ (right), and WaterShed™ with 0.05% (w/v) MWCNTs (left). Note the decrease in plastic region of the nanocomposite specimens when compared to pure WaterShed™

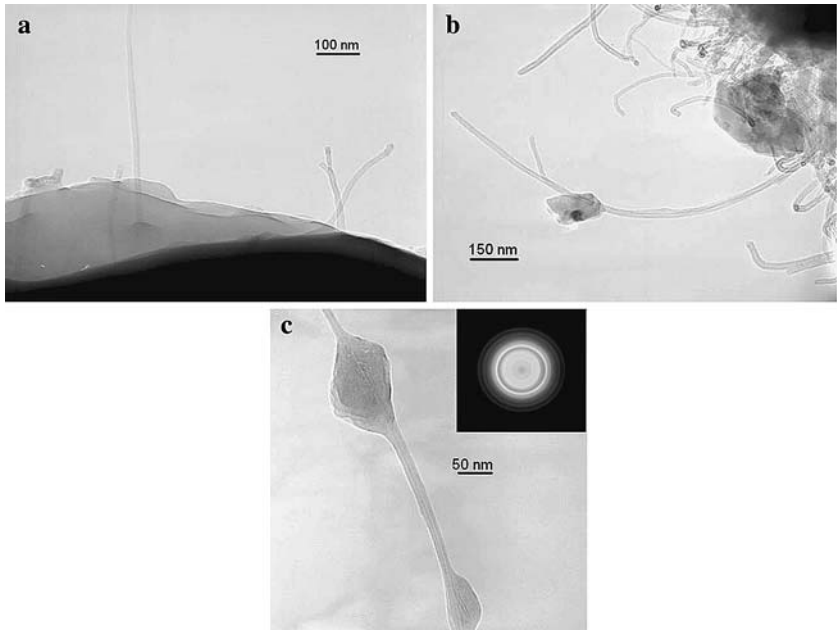

Fig. 10 TEM micrographs taken from the fracture surface of the MWCNTs/SL resin nanocomposite test specimen (**a**, **b** & **c**)

sliced and sandwiched between two 75 square mesh, copper grids and observed in the TEM. These TEM micrographs (Fig. 10 a, b and c) show the affinity between the polymeric matrix and the filler. It can be noted that there is good wetting and a strong interfacial bonding between the materials. MWCNTs/matrix pullout effects were not observed during the TEM characterization process. Pullout effects are mainly observed and attributed to a weak MWCNT interface bonding with the polymer matrix. This poor interfacial bonding results in an actual decrease of the mechanical properties of the pure material [7, 18–20].

A very interesting phenomenon was observed in several micrographs of samples that were previously pulled in tensile tests. The TEM micrographs demonstrate the MWCNT buckling and collapsing effects (Fig. 11) observed in several sections of the samples. These effects are attributed to two main sources: photopolymerization (in the SL machine and in the UV oven), and thermal effects introduced by the SL system's laser as well as the TEM's electron beam. Buckling and collapsing effects of MWCNTs have been previously studied by Wagner et al. (1998). This group characterized an epoxy-based resin that contained MWCNTs under TEM. Wagner's group noticed that the nanotubes buckled and collapsed following the polymerization process of the resin. Furthermore, it was found that mechanical and thermal stresses arising from the polymerization process along with the thermal effects associated with the TEM's electron beam produced this particular phenomenon [1].

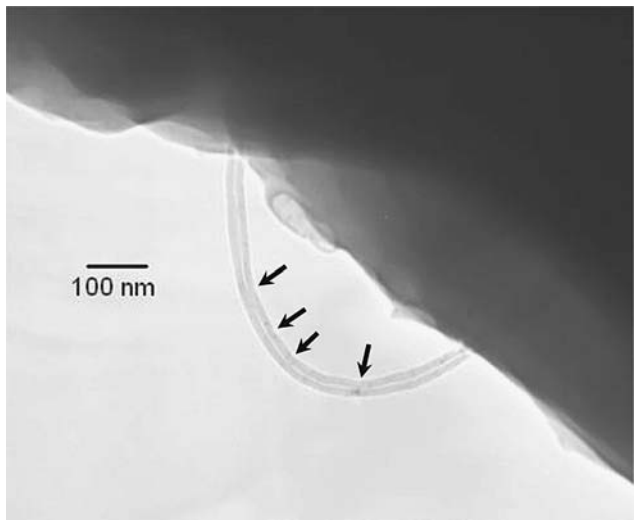

Fig. 11 Buckled MWCNT at the fracture surface of the nanocomposite

Wagner group estimated these stresses to be between 100–150 GPa [1]. The buckling phenomenon observed in the samples supports the idea that there is a strong interface and affinity between the polymeric matrix and the nanotubes. Thus, an effective load transfer from the polymer matrix to the nanotubes exists and therefore, there has been an effective reinforcement of the polymer by introduction of the MWCNTs. More importantly, these hypotheses are supported at the macroscopic level as an improvement in the mechanical properties when compared to unfilled SL resin was observed in the present study.

Complex 3D part demonstration

To demonstrate the functionality of the previously described multi-material SL setup and this novel nanocomposite, a complex 3D geometry was manufactured. A chess rook which is characterized by many intricate and fine details and is a common part manufactured by many SL users (to demonstrate the capabilities of this RP technology) was selected for demonstration. During the building process, the chess rook was visually inspected to ensure that no part delamination or other part distortions were occurring. The approximate build time for a 1″ high rook was ~3 h. Once the part was completed, the part was removed from the platform, cleaned with isopropyl alcohol and postcured for ~30 min in a UV oven. The final product can be observed in Fig. 12 [10].

Conclusions

Novel nanocomposite materials consisting of a photocurable SL epoxy-based matrix and a nanostructured filler material were successfully produced. Complex 3D geometries were successfully fabricated by means of a modified multi-material SL system. The use of MWCNTs as a reinforcement material for WaterShed™ at a concentration of 0.05% (w/v) resulted in an increase of the ultimate tensile strength, fracture strength, and hardness. Moreover, a MWCNT concentration of 0.5% (w/v) in WaterClear™ increased the elastic modulus at temperatures beyond ~200 °C. The 3D random orientation and distribution of the nanotubes allows the user to obtain isotropic properties in the specimens regardless of the orientation on which they are built. These enhancements could result in a new class of high performance SL materials for specific functional applications. Furthermore, these improvements could open new markets and applications for SL and other RP technologies.

An advantage of the non-localized ultrasonic dispersion utilized during this research is that this method does not physically and thus negatively affect the structure of the nanotubes. Electron microscopy showed affinity between the nanocomposite's constituents and strong interfacial bonding effects (buckled nanotubes) were also observed. These effects were reflected at a macroscopic level as an improvement of the mechanical properties when compared to unfilled SL resin. The modified SL machine setup used to manufacture the test specimens and sample parts, allows for testing of a variety of SL resins, nanostructured materials and concentrations without the need for large amounts of materials. The proposed techniques will allow for the future tailoring of the physical properties of SL nanocomposites at large scales.

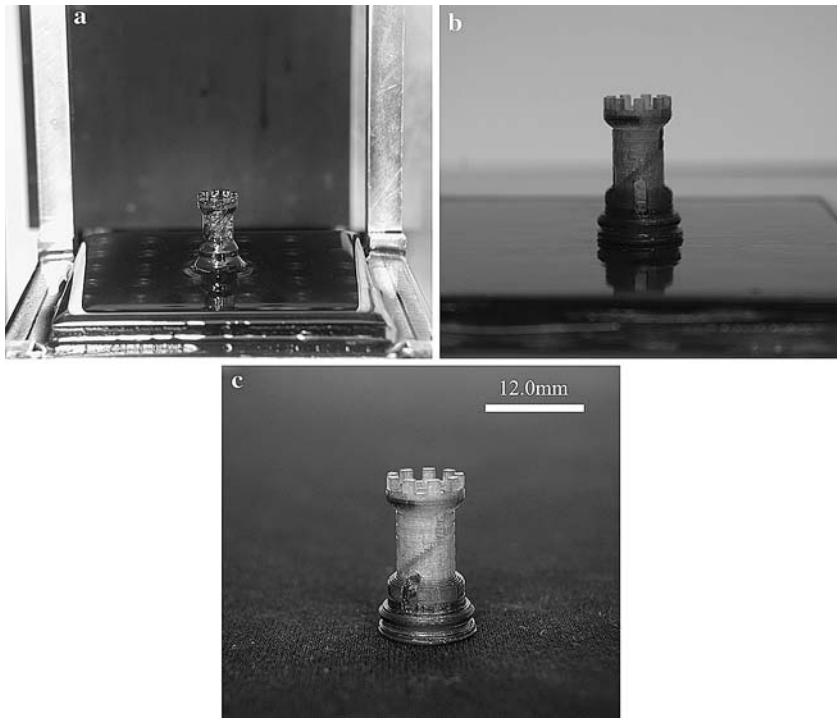

Fig. 12 Building the chess rook on an intermediate resin platform: (**a**) the resin platform, (**b**) the part attached to the intermediate resin platform via a Mylar sheet, and (**c**) the final product

Acknowledgements This research was supported in part by the National Science Foundation, Louis Stokes Alliance for Minority Participation (LSAMP) Bridge to Doctorate Fellowship (JHS and KFS). The research presented here was performed at UTEP in the W.M. Keck Border Biomedical Manufacturing and Engineering Laboratory (W.M. Keck BBMEL) using equipment purchased through Grant # 11804 from the W.M. Keck Foundation. This material is based in part upon work supported by the Texas Advanced Research (Advanced Technology/Technology Development and Transfer) Program under Grant Number 003661-0020-2003. Support was also provided through the Mr. and Mrs. MacIntosh Murchison Chairs No. 1 and 2 (RBW and LEM, respectively).

References

1. Harris P (1999) Carbon nanotubes and related structures. Cambridge University Press, UK
2. Curran SA, Ajayan PM, Blau WJ, Carrol DL, Coleman JN, Dalton AB, Davey AP, Drury A, McCarthy B, Maier S, Strevens AA (1998) Adv Mater 10:1091
3. Andrews R, Wiesenberger MC (2004) In: Carbon nanotube polymer composites, current opinion in solid state and materials science, vol 8. pp 31–37
4. Song YS, Youn JR (2005) Carbon 43(7):1378
5. Sandler J, Shaffer MSP, Prasse T, Bauhofer W, Schulte K, Windle AH (1999) Polymer 40:5967
6. Biercuk MJ, Llagunp MC, Radosavlejevic M, Hyunn JK, Johnson AT (2002) Appl Phys Lett 43:3247
7. Gojny FH, Nastalczyk J, Roslaniec Z, Schulte K (2003) Chem Phys Lett 370:820
8. Jacobs PF (1996) Stereolithography and other RP & M technologies. ASME, New York, New York
9. Jacobs PF (1992) RP & M technologies: fundamentals of stereolithography. SME, Dearborn, Michigan
10. Sandoval JH, Ochoa L, Hernandez A, Soto KF, Murr LE, Wicker RB (2005) In: Proceedings of the 16th Annual Solid Freeform Fabrication Symposium, University of Texas at Austin, August 2005
11. Sandoval JH, Wicker RB (2006) Rapid Prototyping J 12(5):292
12. Lozoya O (2005) Development of a retrofitted multiple material stereolithography system and its use on the characterization of certain multiple material interface mechanical properties. University of Texas at El Paso, Department of Mechanical and Industrial Engineering, Master's Thesis
13. Gojny FH, Wichmann MHG, Fiedler B, Schulte K (2004) Composites Sci Technol 64:2363
14. Ranade AV (2005) In: Microstereolithography of embedded micro-channels. University of Texas at El Paso, Department of Mechanical and Industrial Engineering, Master's Thesis
15. Barpanda D, Mantena PR (1996) J Reinforced Plastics Composites 15:497
16. Sumita M, Tsukihi H, Miyasaka K, Ishikawa K (1984) J Polym Sci 29:1523
17. American Society for Testing Materials (1998) Annual book of ASTM standards, Standard E 1640-99. ASTM, PA pp 689–693
18. American Society for Testing and Materials (1995) Annual book of ASTM standards, Standard D 638-94b. ASTM, PA pp 47–57
19. Davis JR (2004) In: Tensile testing, ASM International, Materials Park, Ohio
20. Jang BZ (2004) In: Advanced polymer composites: principles and applications, ASM International, Materials Park, Ohio
21. Menard K (1999) In: Dynamic mechanical analysis, a practical introduction, CRC, Florida